J|A|C|S
ARTICLES
Published on Web 03/08/2003

Configurational Entropy and Cooperativity between Ligand Binding and Dimerization in Glycopeptide Antibiotics

Sutjano Jusuf,[†] Patrick J. Loll,[‡] and Paul H. Axelsen*,[†]

Contribution from the Department of Pharmacology, University of Pennsylvania, Philadelphia, Pennsylvania 19104, and Department of Biochemistry, Medical College of Pennsylvania−Hahnemann University, Philadelphia, Pennsylvania 19102

Received July 19, 2002; E-mail: axe@pharm.med.upenn.edu

Abstract: Oligomerization and ligand binding are thermodynamically cooperative processes in many biochemical systems, and the mechanisms giving rise to cooperative behavior are generally attributed to changes in structure. In glycopeptide antibiotics, however, these cooperative processes are not accompanied by significant structural changes. To investigate the mechanism by which cooperativity arises in these compounds, fully solvated molecular dynamics simulations and quasiharmonic normal-mode analysis were performed on chloroeremomycin, vancomycin, and dechlorovancomycin. Configurational entropies were derived from the vibrational modes recovered from ligand-free and ligand-bound forms of the monomeric and dimeric species. Results indicate that both ligand binding and dimerization incur an entropic cost as vibrational activity in the central core of the antibiotic is shifted to higher frequencies with lower amplitudes. Nevertheless, ligand binding and dimerization are cooperative because the entropic cost of both processes occurring together is less than the cost of these processes occurring separately. These reductions in configurational entropy are more than sufficient in magnitude to account for the experimentally observed cooperativity between dimerization and ligand binding. We conclude that biochemical cooperativity can be mediated through changes in vibrational activity, irrespective of the presence or absence of concomitant structural change. This may represent a general mechanism of allostery underlying cooperative phenomena in diverse macromolecular systems.

Introduction

Glycopeptide antibiotics bind stereospecifically to target ligands in bacterial cell walls,[1] and they form asymmetric homodimers.[2,3] In general, ligand binding promotes dimerization, and vice versa.[4−6] Mechanistic explanations for this cooperative behavior tend to focus on the extensive hydrogen-bond networks across the dimer interface and the ligand−antibiotic interfaces (Figure 1). For example, it has been suggested that hydrogen bonding across the dimeric interface induces hyperpolarization of the amide groups and that this hyperpolarization may strengthen hydrogen bonds across the ligand−antibiotic interface.[7] Recent proton NMR studies have been interpreted as showing that these interfaces "tighten" in a cooperative manner.[8] It has also been suggested that cooperativity is a direct result of electrostatic effects.[4,5] These explanations imply that enthalpy changes, rather than entropy changes, have a dominant role in the thermodynamics of cooperativity.

Alternative explanations for cooperativity that assign a dominant role to entropy changes have also been suggested. For example, dimerization may suppress structural fluctuations of the antibiotic and stabilize a subset of structures in which the binding site is more favorable for ligand binding.[4] Alternatively, local changes in vibrational activity may exert allosteric effects that are also manifested as changes in vibrational activity. Theoretical[9] and experimental[10,11] support for the operation of this mechanism in other systems has been presented, and a preliminary report suggesting that vibrational entropy mediates cooperativity in glycopeptide antibiotics has been published.[12]

Discerning the relative importance of enthalpy and entropy changes to the cooperative relationship between two processes is difficult because structural changes are more easily measured by experimental methods, and they can be characterized in greater detail. Consequently, structural changes tend to obscure and draw attention away from any role that entropy changes

* To whom correspondence should be addressed: Tel (215) 898-9238.
[†] University of Pennsylvania.
[‡] Hahnemann University.

(1) Loll, P. J.; Axelsen, P. H. *Annu. Rev. Biophys. Biophys. Struct.* **2000**, *29*, 265−289.
(2) Groves, P.; Searle, M. S.; Mackay, J. P.; Williams, D. H. *Structure* **1994**, *2*, 747−753.
(3) Sheldrick, G. M.; Paulus, E.; Vertesy, L.; Hahn, F. *Acta Crystallogr.* **1995**, *B51*, 89−98.
(4) Mackay, J. P.; Gerhard, U.; Beauregard, D. A.; Maplestone, R. A.; Williams, D. H. *J. Am. Chem. Soc.* **1994**, *116*, 4573−4580.
(5) Mackay, J. P.; Gerhard, U.; Beauregard, D. A.; Westwell, M. S.; Searle, M. S.; Williams, D. H. *J. Am. Chem. Soc.* **1994**, *116*, 4581−4590.
(6) McPhail, D.; Cooper, A. *J. Chem. Soc., Faraday Trans.* **1997**, *93*, 2283−2289.
(7) Loll, P. J.; Bevivino, A. E.; Korty, B. D.; Axelsen, P. H. *J. Am. Chem. Soc.* **1997**, *119*, 1516−1522.
(8) Calderone, C. T.; Williams, D. H. *J. Am. Chem. Soc.* **2001**, *123*, 6262−6267.
(9) Cooper, A.; Dryden, D. T. F. *Eur. Biophys. J.* **1984**, *11*, 103−109.
(10) Maler, L.; Blankenship, J.; Rance, M.; Chazin, W. J. *Nat. Struct. Biol.* **2000**, *7*, 245−250.
(11) Palmer, A. G. *Annu. Rev. Biophys. Biomol. Struct.* **2001**, *30*, 129−155.
(12) Jusuf, S.; Loll, P. J.; Axelsen, P. H. *J. Am. Chem. Soc.* **2002**, *124*, 3490−3491.

10.1021/ja027780r CCC: $25.00

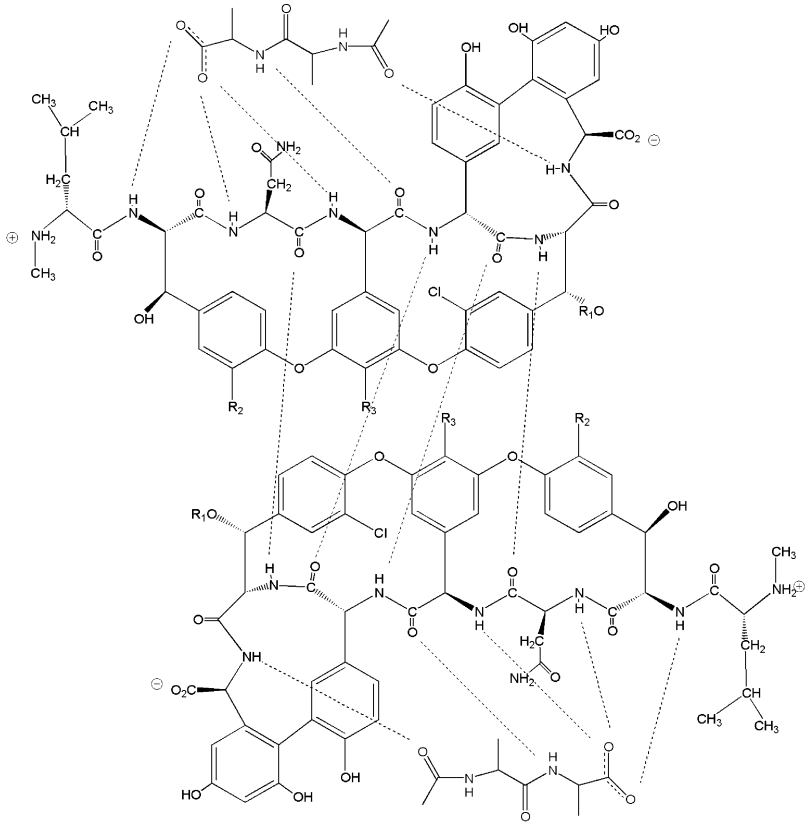

	R_1	R_2	R_3
Vancomycin	H	Cl	L-vancosamine, D-glucose
Dechlorovancomycin	H	H	L-vancosamine, D-glucose
Chloroeremomycin	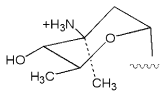	Cl	4-epi-L-vancosamine, D-glucose

Figure 1. Schematic representation of the binding interfaces in the three glycopeptide antibiotics.

may have in mediating cooperativity. When the role of entropy changes is unknown, one cannot be certain that structural changes are mechanistically responsible for cooperativity.

The studies described herein were prompted by the observation that dimerization and ligand binding tend to be highly cooperative in glycopeptide antibiotics despite high-resolution crystallographic studies indicating that significant structural changes do not occur.[3,7,12−18] These are remarkable circumstances because they appear to require an entropic mechanism to explain cooperative behavior. Studies of these complexes, therefore, offer a unique opportunity to determine whether entropy changes, occurring in the absence of structural changes, can account for the cooperative relationship between these processes. The present study examines this question in three glycopeptide antibiotics, chloroeremomycin (CEM), vancomycin (VMN), and dechlorovancomycin (DCV), using fully solvated molecular dynamics simulations and quasiharmonic normal-mode analysis to calculate the changes in configurational entropy that occur upon dimerization and the binding of the ligand acetyl-D-alanyl-D-alanine (AcDADA). Two manifestations of

(13) Schafer, M.; Pohl, E.; SchmidtBase, K.; Sheldrick, G. M.; Hermann, R.; Malabarba, A.; Nebuloni, M.; Pelizzi, G. *Helv. Chim. Acta* **1996**, *79*, 1916−1924.
(14) Schafer, M.; Schneider, T. R.; Sheldrick, G. M. *Structure* **1996**, *4*, 1509−1515.
(15) Loll, P. J.; Miller, R.; Weeks, C. M.; Axelsen, P. H. *Chem. Biol.* **1998**, *5*, 293−298.
(16) Schafer, M.; Sheldrick, G. M.; Schneider, T. R.; Vertesy, L. *Acta Crystallogr.* **1998**, *D54*, 175−183.
(17) Loll, P. J.; Kaplan, J.; Selinsky, B. S.; Axelsen, P. H. *J. Med. Chem.* **1999**, *42*, 4714−4719.
(18) Kaplan, J.; Korty, B. D.; Axelsen, P. H.; Loll, P. J. *J. Med. Chem.* **2001**, *44*, 1837−1840.

cooperativity are explicitly considered: that occurring between dimerization and ligand binding and that occurring between the two ligand binding sites in a dimer.

Methods

Nomenclature. The antibiotics in this study form asymmetric dimers as a consequence of the disaccharide group orientation.[1] We have adopted a convention whereby the vancomycin unit with the terminal vancosamine sugar residue overlying the ligand-binding site is denoted as V_I, while its counterpart is denoted as V_{II}. An AcDADA ligand is denoted as L. A center dot between two entities represents a binding interface. Hence, the notations $L{\cdot}V_I$ and $L{\cdot}V_{II}$ refer to ligand-bound monomers of vancomycin, while $V_I{\cdot}V_{II}$ denotes the ligand-free vancomycin dimer. Chloroeremomycin and dechlorovancomycin monomers are named analogously to vancomycin with letters C and D, respectively, instead of V. M will be a generic symbol used to indicate any one of the three antibiotic monomers.

Simulation Specifications. Energy minimizations and dynamics simulations were performed with CHARMM[19] version c27b2 on a 32 × 800 MHz Intel PIII cluster with a Myrinet switch. Atom types and all-hydrogen parameters were described previously.[20−22] Electrostatic interactions were computed with the particle mesh Ewald (PME) algorithm with a β-spline order of 6, FFT grid of one point per (64 × 64 × 64) Å and a real space Gaussian-width κ of 0.4 Å^{-1}.[23] The nonbonded van der Waals interactions was truncated at 12 Å, with an atom-based cutoff. Dynamic trajectories were generated at a constant pressure and temperature (1.0 atm and 300 K).[24,25] The SHAKE algorithm[26] was used to constrain bond distances to hydrogen atoms during dynamics, and the equation of motion was integrated with a time step of 1 fs.

System Specifications. A model of the crystalline vancomycin·acetate complex was developed to validate the simulation parameters by comparison with the 0.89 Å crystallographic structure of Protein Data Bank entry 1AA5.[7] The final model had unit cell dimensions of 28.81, 28.81, and 66.13 Å at room temperature, making its unit cell volume 54 889 Å^3. The system contained 43 waters identified in the crystal structure, 83 additional waters, and three sodium ions in each of eight asymmetric dimeric units in the unit cell. All of the carboxylate groups were ionized.

In simulations prepared for quasiharmonic analysis, a doubly liganded dimeric complex of each antibiotic was placed in a cubic 40 Å periodic boundary. Initial coordinates for the $L{\cdot}V_I{\cdot}V_{II}{\cdot}L$ complex were generated by docking two AcDADA ligands into dimeric vancomycin derived from the crystal structure 1AA5. From this structure, the $L{\cdot}D_I{\cdot}D_{II}{\cdot}L$ complex was created by replacing the chlorine on residue 2 with a hydrogen, and the $L{\cdot}C_I{\cdot}C_{II}{\cdot}L$ complex was generated by adding a vancosamine residue to a vancomycin dimer such that two additional H-bonds form across the dimeric interface.[27] This results in a model of CEM with L-vancosamine instead of 4-*epi*-L-vancosamine, but it avoids perturbation of the crystallographically determined disaccharide structure on residue 4. Varying numbers of chloride ions were added for charge balance and placed at positions consistent with those found in the reference crystal coordinate (Table 1).

Structure Preparation and Conditioning. The three doubly liganded complexes were then energy-minimized for 2000 steps by the adapted basis Newton−Raphson method with all atoms constrained except the ligands and the asparagine side chain (the latter partially occupies the ligand-binding site of V1 but not V2 in the 1AA5 crystal structure). Each system was propagated for 5 ps at 300 K and then for another 5 ps at 150 K while the complexes were constrained to their initial coordinates. From 10 to 22 ps each system was heated incrementally (200, 225, 250, 275, 300, and 320 K) and random velocity assignments were applied every 0.2 ps.[28] From 22 to 40 ps the systems were cooled to 300 K while random velocity assignments continued at every 0.2 ps. After this 40-ps conditioning period, no constraints other than SHAKE and no external interventions were applied as the simulations propagated to 1700 ps. The final coordinates from these three doubly liganded dimeric systems were then used to generate the 24 complexes in which binding cooperativity was examined (Table 1). Seven additional simulation systems representing every possible combination of monomeric unit and ligand (i.e., M_I, M_{II}, $M_I{\cdot}M_{II}$, $M_I{\cdot}L$, $M_{II}{\cdot}L$, $L{\cdot}M_I{\cdot}M_{II}$, and $M_I{\cdot}M_{II}{\cdot}L$) were prepared by deleting monomeric units, ligands, and chloride ions from each of the three doubly liganded dimeric systems. After these deletions, a 40 × 40 × 40 Å cubic array of water molecules was overlaid on each system and waters within 2.8 Å of any system component were deleted. The final compositions of the 24 systems generated in this manner are summarized in Table 1.

Each system was propagated for 10 ps at 300 K with nonsolvent atoms constrained. From 10 to 100 ps harmonic constraints were applied to all non-hydrogen nonsolvent atoms and tapered to zero. From that point, all systems were propagated for 900 ps with SHAKE as the only constraint, for a total simulation length of 1000 ps. Coordinates were saved every 50 fs.

Quasiharmonic Normal-Mode Analysis. Vibrational analysis was performed on the 65 non-hydrogen atoms that comprise a macrocyclic core common to all three antibiotics (Figure 3), by use of the VIBRAN utility in CHARMM.[29] This set of atoms was chosen so that modes recovered are comparable across the three compounds and to facilitate

Table 1. Atom Counts in the 24 Systems Studied[a]

systems	glycopeptide and ligand atoms	chloride ions	water molecules	total atoms
D_I	177	1	2057	6349
D_{II}	177	1	2054	6340
$L{\cdot}D_I$	204	0	2051	6357
$L{\cdot}D_{II}$	204	0	2048	6348
$D_I{\cdot}D_{II}$	354	2	1944	6188
$L{\cdot}D_I{\cdot}D_{II}$	381	1	1937	6193
$D_I{\cdot}D_{II}{\cdot}L$	381	1	1938	6196
$L{\cdot}D_I{\cdot}D_{II}{\cdot}L$	408	0	1931	6201
V_I	177	1	2061	6361
V_{II}	177	1	2063	6367
$L{\cdot}V_I$	204	0	2058	6378
$L{\cdot}V_{II}$	204	0	2061	6387
$V_I{\cdot}V_{II}$	354	2	1953	6215
$L{\cdot}V_I{\cdot}V_{II}$	381	1	1950	6232
$V_I{\cdot}V_{II}{\cdot}L$	381	1	1951	6235
$L{\cdot}V_I{\cdot}V_{II}{\cdot}L$	408	0	1948	6252
C_I	201	2	2042	6329
C_{II}	201	2	2040	6323
$L{\cdot}C_I$	228	1	2035	6334
$L{\cdot}C_{II}$	228	1	2035	6334
$C_I{\cdot}C_{II}$	402	4	1927	6187
$L{\cdot}C_I{\cdot}C_{II}$	429	3	1920	6192
$C_I{\cdot}C_{II}{\cdot}L$	429	3	1922	6198
$L{\cdot}C_I{\cdot}C_{II}{\cdot}L$	456	2	1915	6203

[a] Dechlorovancomycin, vancomycin, and chloroeremomycin monomers have +1, +1, and +2 charges, respectively. the ligand AcDADA is negatively charged at neutral conditions. The number of chloride ions was varied to achieve charge balance.

(19) Brooks, B. R.; Bruccoleri, R. E.; Olafson, B. D.; States, D. J.; Swaminathan, S.; Karplus, M. *J. Comput. Chem.* **1983**, *4*, 187−217.
(20) Li, D.; Sreenivasan, U.; Juranic, N.; Macura, S.; Puga, F. J., II; Frohnert, P. M.; Axelsen, P. H. *J. Mol. Recog.* **1997**, *10*, 73−87.
(21) Axelsen, P. H.; Li, D. *Bioorg. Med. Chem.* **1998**, *6*, 877−881.
(22) Axelsen, P. H.; Li, D. *J. Comput. Chem.* **1998**, *19*, 1278−1283.
(23) Essmann, U.; Perera, L.; Berkowitz, M. L.; Darden, T.; Lee, H.; Pedersen, L. G. *J. Chem. Phys.* **1995**, *103*, 8577−8593.
(24) Nose, S.; Klein, M. L. *Mol. Phys.* **1983**, *50*, 1055−1076.
(25) Feller, S. E.; Zhang, Y.; Pastor, R. W.; Brooks, B. R. *J. Chem. Phys.* **1995**, *103*, 4613−4621.
(26) Ryckaert, J. P.; Ciccotti, G.; Berendsen, H. J. C. *J. Comput. Phys.* **1977**, *23*, 327−341.
(27) Waltho, J. P.; Williams, D. H. *J. Am. Chem. Soc.* **1989**, *111*, 2475−2480.
(28) Northrup, S. H.; Pear, M. R.; Morgan, J. D.; McCammon, J. A.; Karplus, M. *J. Mol. Biol.* **1981**, *153*, 1087−1109.

an accurate diagonalization of the 195 × 195 mass-weighted atomic position displacement covariance matrix. Prior to diagonalization, coordinates of the macrocycle core from the trajectory were reoriented by minimizing their mass-weighted root-mean-square difference with respect to the average structure. This negated overall translation and rotation, resulting in six null frequencies corresponding to translational and rotational degrees of freedom and 189 vibrational modes. Vibrational entropy was calculated at 300 K from the recovered modes by use of the ordinary vibrational partition function[30]

$$TS_{\mathrm{vib},i} = k_{\mathrm{B}}T\frac{\Theta}{\mathrm{e}^{\Theta}-1} + k_{\mathrm{B}}T\ln\left(\frac{1}{1-\mathrm{e}^{-\Theta}}\right)$$

and

$$\Theta = \frac{h\omega_i c}{k_{\mathrm{B}}T}$$

where h is Plank's constant, c is the speed of light, and ω_i is the ith frequency in reciprocal centimeters.

Results

Parameter Validation. A whole-crystal 1200 ps simulation of the vancomycin·acetate complex was performed and compared to the 0.89 Å crystallographic structure of Protein Data Bank entry 1AA5[7] to validate the simulation parameters. This task was not straightforward because the unit cell is large, and most portions of the crystal other than vancomycin itself consist of disordered solvent and an indeterminate number of sodium counterions.

Our goal was to demonstrate whether an unconstrained full crystal simulation could be performed at constant temperature and pressure that faithfully preserves the original crystal structure and unit cell dimensions. This goal was ultimately achieved by systematically varying the number of water molecules in a CPT (constant pressure and temperature) simulation with periodic boundaries until a system was found that faithfully maintained the correct unit cell volume. The published unit cell dimensions of 28.45, 28.45, and 65.84 Å pertain to 98 K.[7] At room temperature these dimensions expand to 28.81, 28.81, and 66.13 Å, yielding a target volume of 6861 Å^3 per dimeric unit (unpublished data).

Figure 2shows a plot of unit cell volume vs simulation time in a full crystal 1200 ps simulation of the crystal structure of vancomycin dimer with a bound acetate ligand, 43 waters observed in the crystal structure, 83 additional waters, and three sodium ions (all carboxylate groups were ionized). The system was preconditioned for 300 ps with rigid unit cell dimensions and harmonic restraints on the position of all atoms with crystallographically determined positions. After 300 ps, the system was propagated under CPT conditions so that the unit cell volume could fluctuate. At 600 ps, harmonic restraints were removed and the system was propagated for an additional 600 ps (total simulation time 1200 ps). A comparison of the instantaneous unit cell volumes to horizontal lines at ±30 Å^3, representing the target unit cell volume for systems with one additional or one less water molecule, suggests that the simulation system has the correct number of water molecules to within ±1 molecule.

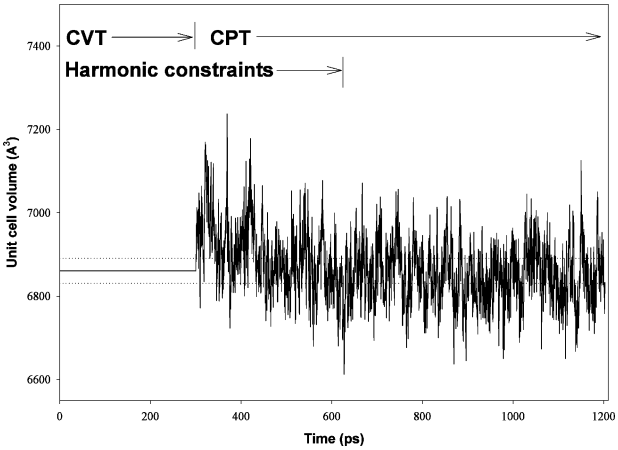

Figure 2. Unit cell volume of a vancomycin crystal simulation. The target volume of the vancomycin crystal system, 6861 A^3, was reproduced by the simulation using the charmm force fields and parameters along with the application of positional harmonic restraints during the initial preconditioning. The first 300 ps were run under conditions of constant volume and temperature (CVT); the remainder of the simulation was run under constant pressure and temperature (CPT) conditions. The solid horizontal line between 0 and 300 ps represents the target unit cell volume per dimeric unit. Dotted lines at ±30 Å^3 show the target unit cell volume for systems with one additional or one less water molecule.

Differences between the average structure calculated over a 300 ps interval (from 900 to 1200 ps) and the crystallographically determined structure were less than the crystallographic resolution of 0.89 Å for 88% of the non-hydrogen atoms (i.e., 184 of 210 atoms, excluding solvent) and less than 1.5 Å for 96% of the non-hydrogen atoms. The largest discrepancies between the simulation-average structure and the crystal structure were invariably in regions of crystal disorder where differences would be expected, i.e., the side chains of residues 1 and 3 and the disaccharide groups. The average RMS fluctuations of macrocycle atoms in the simulation (∼0.23 Å^2) corresponds closely to the mean fluctuations derived from the temperature factor of the crystal (∼0.18 Å^2).

In sum, these results demonstrate that the models and parameters used in these unrestrained simulations of the crystalline vancomycin dimer yield a system in which unit cell dimensions, atomic positions, and positional fluctuation magnitudes are in excellent agreement with experimental results.

Conformational Consequences of Ligand Binding and Dimerization. The macrocyclic rings of each antibiotic exhibited considerable structural flexibility in simulations (Figure 3). Nevertheless, the macrocyclic core maintained a well-defined and generally uniform conformation regardless of dimerization or the presence of ligand. The largest RMS structural change induced by ligand binding or dimerization for the 65-atom core structure was 0.35 Å, which is comparable to the largest RMS difference seen between any two monomers in any given X-ray crystal structure.[15,17] By this measure, the consequences of ligand binding and dimerization on the average conformation of a glycopeptide antibiotic are small.

Dynamics Analysis. Both ligand binding and dimerization tended to reduce the amplitude of structural fluctuations. For example, RMS fluctuations (second moment) for the 65 core macrocycle atoms in the ligand-free C_I monomer were 0.44 Å over the 800 ps interval from 200 to 1000 ps. These fluctuations decreased to 0.29 Å in the C_I·C_{II} dimer and to 0.30 Å in the L·C_I complex over the same interval. Upon dimerization and

(29) Brooks, B. R.; Janezic, D.; Karplus, M. *J. Comput. Chem.* **1995**, *16*, 1522−1542.
(30) McQuarrie, D. A. *Statistical Mechanics*; Harper & Row: New York, 1976.

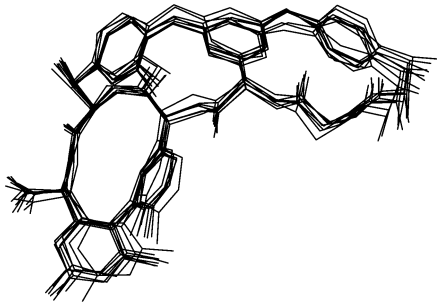

Figure 3. Macrocycle dynamics. Seven superimposed snapshots of the dechlorovancomycin macrocycles over an 800 ps interval show that significant fluctuations occur while a single overall conformation is retained. These coordinates were extracted from a simulation of the dechlorovancomycin dimer that included all hydrogens, 1944 waters, and two chloride ions for a total of 6188 atoms in each periodically bounded cell.

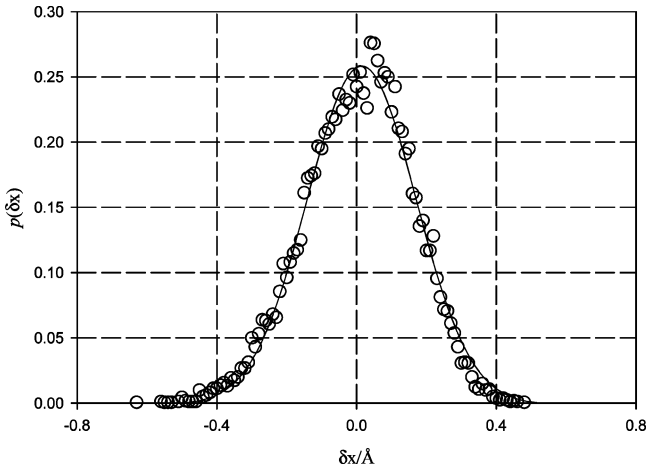

Figure 4. Histogram of the probability distribution of one coordinate of a macrocycle atom with a skew of 0.2. The mean position of an atom along its principal *x*-axis was determined, and the deviation of the atom position from this mean was calculated at every 50 fs during the final 800 ps simulation of the chloroeremomycin monomer, E1. Circles represent the normalized probability of a deviation collected into 0.05 Å bins. This atom and this axis were chosen to illustrate the shape of a distribution that has a skew value of 0.2. For comparison, a solid line representing a normal distribution with no skew has been fit to the data.

ligand binding, the fluctuations of C_I in the $L{\cdot}C_I{\cdot}C_{II}$ complex decreased further to 0.25 Å. These motions exhibit relatively little skew, with an average third moment magnitude of ~0.2 (Figure 4). Therefore, one may reasonably estimate the thermodynamic consequences of fluctuation amplitude reduction by applying quasiharmonic normal-mode analysis to obtain vibrational frequencies and converting these frequencies into entropy units (see Methods).

Analysis of the 800 ps interval from 200 to 1000 ps for the 65 core macrocycle atoms yielded 189 vibrational modes in each monomer with frequencies ranging from 6 to 2800 cm^{-1}. Ligand binding and dimerization broadly increased the frequencies of lower frequency modes up to 650 cm^{-1}. Particular attention was given to the lowest frequency modes because they make the largest contribution to configurational entropy and are associated with the largest amplitude motions. It is unlikely that vibrational modes with frequencies lower than 6 cm^{-1} were present because the Nyquist critical frequency is 0.02 cm^{-1} for an 800 ps interval. The lowest vibrational modes of each monomeric species ranged from 6 to 9 cm^{-1}, and their eigenvectors exhibited an interesting pattern of overlap (Table 2). In each case, the overlap is greater for corresponding monomers of two

Table 2. Lowest Quasiharmonic Modes and Their Eigenvectors Overlap for the Unbound Monomers

monomers	lowest quasiharmonic mode (cm^{-1})	overlap D_I	D_{II}	V_I	V_{II}	C_I	C_{II}
D_I	8.46	1.0					
D_{II}	6.08	0.74	1.0				
V_I	6.46	0.91	0.44	1.0			
V_{II}	6.04	0.61	0.93	0.33	1.0		
C_I	7.31	0.92	0.76	0.95	0.50	1.0	
C_{II}	6.25	0.54	0.91	0.22	0.96	0.45	1.0

Table 3. Vibrational Entropy of Monomers with Respect to Their Undimerized Ligand-Free State[a]

	complex	chloroeremomycin C_I	chloroeremomycin C_{II}	vancomycin V_I	vancomycin V_{II}	dechlorovancomycin D_I	dechlorovancomycin D_{II}
1	$L{\cdot}M_I$	−21		−16		−17	
2	$L{\cdot}M_{II}$		−19		−17		−22
3	$M_I{\cdot}M_{II}$	−25	−26	−2	−13	−2	−15
4	$L{\cdot}M_I{\cdot}M_{II}$	−34	−27	−17	−12	−15	−7
5	$M_I{\cdot}M_{II}{\cdot}L$	−24	−33	−1	−22	−6	−27
6	$L{\cdot}M_I{\cdot}M_{II}{\cdot}L$	−34	−33	−15	−23	−22	−30

[a] Units are $T\Delta S$ in kilojoules per mole at 300 K, and their precision is estimated to be ±2 kJ/mol (see Results).

different antibiotic species (e.g., C_{II} and D_{II}) than for monomers of the same species but with different sugar orientations (e.g., C_I and C_{II} or D_I and D_{II}). This is significant because it indicates that disaccharide orientation alters the character of macrocycle dynamics. Therefore, configurational entropies derived from quasiharmonic analysis will be influenced by disaccharide orientation even though the disaccharide groups are not in the set of 65 core macrocycle atoms subjected to this analysis.

Cooperativity. We define cooperativity in terms of the following set of competitive binding equilibria:

interprocess cooperativity, M_I	$L{\cdot}M_I + M_I{\cdot}M_{II} \rightleftharpoons L{\cdot}M_I{\cdot}M_{II} + M_I$
interprocess cooperativity, M_{II}	$L{\cdot}M_{II} + M_I{\cdot}M_{II} \rightleftharpoons M_I{\cdot}M_{II}{\cdot}L + M_{II}$
intraprocess cooperativity	$L{\cdot}M_I{\cdot}M_{II} + M_I{\cdot}M_{II}{\cdot}L \rightleftharpoons L{\cdot}M_I{\cdot}M_{II}{\cdot}L + M_I{\cdot}M_{II}$
overall cooperativity	$L{\cdot}M_I + M_{II}{\cdot}L + M_I{\cdot}M_{II} \rightleftharpoons L{\cdot}M_I{\cdot}M_{II}{\cdot}L + M_I + M_{II}$

where M represents monomeric CEM, VMN, or DCV, the subscripts reference the nonidentical "sides" of a dimeric complex as defined above, L represents the ligand, and positive cooperativity is an energetic preference for the right-hand side. The first two equilibria describe competition between dimerization and ligand binding, and therefore they are designated "interprocess" cooperativities (Table 4). The third equilibrium describes the effect of one ligand on the binding of another, and is therefore designated "intraprocess" cooperativity (Table 5). The sum of these three equilibria yields an overall cooperativity (Table 6) between ligand binding and dimerization. Note that the loss of ligand entropy upon binding does not enter into these definitions. Also note that the amount of monomeric and dimeric antibiotic is identical on both sides of all equilibria. Therefore, the entropy losses due to immobilization of the disaccharide units upon dimerization cancel.

With respect to configurational entropy, our results indicate that CEM, VMN, and DCV have overall cooperativities of +24, +10, and +4 kJ/mol. The values for CEM and VMN differ slightly from our previously reported values of +25 and +9 kJ/mol because the set of core macrocycle atoms was defined differently (the current analysis excluded the chlorine atom on residue 2 that is not present in DCV). The experimentally

Table 4. Interprocess Cooperativities[a]

	process	C_I	C_{II}	V_I	V_{II}	D_I	D_{II}
1	$M_I{\cdot}M_{II} \rightarrow M_I + M_{II}$	25	26	2	13	2	15
	Side 1						
2	$L{\cdot}M_I \rightarrow L + M_I$	21	0	16	0	17	0
3	$L + M_I + M_{II} \rightarrow L{\cdot}M_I{\cdot}M_{II}$	−34	−27	−17	−12	−15	−7
	$L{\cdot}M_I + M_I{\cdot}M_{II} \rightarrow L{\cdot}M_I{\cdot}M_{II} + M_I$ (sum of rows 1−3)	+12	**−1**	+1	+1	+4	+8
	Side 2						
4	$L{\cdot}M_{II} \rightarrow L + M_{II}$	0	19	0	17	0	22
5	$M_I + M_{II} + L \rightarrow M_I{\cdot}M_{II}{\cdot}L$	−24	−33	−1	−22	−6	−27
	$L{\cdot}M_{II} + M_I{\cdot}M_{II} \rightarrow M_I{\cdot}M_{II}{\cdot}L + M_{II}$ (sum of rows 1, 4, and 5)	+1	+12	+1	+8	−4	+10

[a] Units are $T\Delta S$ in kilojoules per mole at 300 K. Data for rows 3 and 5 are derived directly from Table 3; the data for rows 1, 2, and 4 are derived from Table 3 by negation.

Table 5. Intraprocess Cooperativities[a]

	process type	C_I	C_{II}	V_I	V_{II}	D_I	D_{II}
1	$M_I + M_{II} \rightarrow M_I{\cdot}M_{II}$	−25	−26	−2	−13	−2	−15
2	$L{\cdot}M_I{\cdot}M_{II} \rightarrow L + M_I + M_{II}$	34	27	17	12	15	7
3	$M_I{\cdot}M_{II}{\cdot}L \rightarrow M_I + M_{II} + L$	24	33	1	22	6	27
4	$L + M_I + M_{II} + L \rightarrow L{\cdot}M_IM_{II}{\cdot}L$	−34	−33	−15	−23	−22	−30
	$L{\cdot}M_I{\cdot}M_{II} + M_I{\cdot}M_{II}{\cdot}L \rightarrow L{\cdot}M_IM_{II}{\cdot}L + M_I{\cdot}M_{II}$ (sum of rows 1−4)	−1	+1	+1	−2	−3	−11

[a] Units are $T\Delta S$ in kilojoules per mole at 300 K. Values for rows 1 and 4 are derived directly from Table 3; the data for rows 2 and 3 are derived from Table 3 by negation.

Table 6. Overall Cooperativities[a]

	process type	C_I	C_{II}	V_I	V_{II}	D_I	D_{II}
1	interprocess cooperativities, side 1	+12	−1	+1	+1	+4	+8
2	interprocess cooperativities, side 2	+1	+12	+1	+8	−4	+10
3	intraprocess cooperativities	−1	+1	+1	−2	−3	−11
	partial cooperativities (sum of rows 1−3)	+12	+12	+3	+7	−3	+7
	overall cooperativity	+24		+10		+4	

[a] Units are $T\Delta S$ in kilojoules per mole at 300 K.

measured cooperativities for CEM, VMN, and DCV from Williams are +11.9, +5.3, and +5.0 kJ/mol.[31] Because these latter values represent overall free energies, they are not directly comparable to the results of configurational entropy calculations. However, it is significant that the calculated results are larger than experimental results, indicating that changes in configurational entropy are more than sufficient to account for the experimentally measured free energy changes associated with cooperativity.

The overall cooperativities of CEM and VMN in terms of configurational entropy (+24 and +10 kJ/mol) are about twice the magnitude of their experimentally determined cooperative free energies, whereas the overall cooperativity for DCV in terms of its configurational entropy (+4 kJ/mol) is about the same as its experimental cooperative free energy. The most likely reason that DCV differs from CEM and VMN in this respect is that it lacks a chlorine atom on residue 2. This atom is a significant point of contact in the dimer interfaces of CEM and VMN. Its absence in DCV alters the interactions and dynamics of the dimer and most likely accounts for the large negative intracooperativity of DCV (Tables 5). Note that ligand binding to D_I in a DCV dimer causes an increase in the configurational entropy of D_{II} (compare rows 3 and 4 of Table 3). Consequently, binding of another ligand by the $L{\cdot}D_I{\cdot}D_{II}$ complex entails a higher entropic cost.

Error Analysis. To assess the precision of our entropic cost results, eight simulations of the $V_I{\cdot}V_{II}$ dimer lasting 1.0 ns each were performed with different initial velocity assignments and starting coordinates. Total configurational entropy determinations for the core macrocycle atoms tended to become more precise and reproducible as simulation time increased, up to about 800 ps. The standard deviation of eight separate determinations was 3.1 kJ/mol for an interval of 300 ps, 2.1 kJ/mol for 500 ps, 1.8 kJ/mol for 800 ps, and 1.9 kJ/mol for 1200 ps. Two different 500 ps time windows (500−1000 and 1000−1500 ps) yielded virtually identical total configurational energies and standard deviations. Thus, we have applied quasiharmonic normal-mode analysis to the final 800 ps of the 1 ns simulations and estimate that the total configurational entropy results reported herein have a standard deviation of 2 kJ/mol.

The inclusion of hydrogen atoms in the vibrational analyses had a negligible impact on final results (<0.5 kJ/mol), most likely because SHAKE constraints remove any fine structure that results from high-frequency hydrogen-stretching vibrations.[32] The motions of the disaccharides and the side chains of residues 1 and 3 were not included in the foregoing analysis. When they were included, cooperativity between ligand binding and dimerization for CEM increased from 24 to 33 kJ/mol (this type of analysis was not done on VMN and DCV). This suggests that the inclusion of anharmonic groups in this analysis would amplify rather than diminish the degree of cooperativity attributable to configurational entropy changes in these systems. However, these motions are severely anharmonic, and the simulation length was insufficient to sample events such as rotation of the side chains and sugar residues. Thus, estimates of configurational entropy in these systems are likely to be inaccurate.

Discussion

These data point to a conclusion that may be summarized in simple terms: ligand binding and dimerization exhibit positive cooperativity in these antibiotics because both processes share a common entropic cost (Figure 5). After one process pays the entropic cost of shifting vibrational activity in the antibiotic to higher frequencies and lower amplitudes, that cost does not have to be paid again by the other process because ligand binding and dimerization are structurally congruent processes, i.e., both processes cause molecules to converge on the same average structure when fluctuation amplitudes are reduced.

When biochemical processes occur in conjunction with structural changes, it is common to explain thermodynamic cooperativity between them solely in terms of the structural change. However, this practice focuses exclusively on changes in system enthalpy, and it implicitly assumes that the cooperative mechanism is enthalpy-driven. In glycopeptide antibiotics, there appears to be no significant structural change associated with ligand binding or dimerization, yet these processes exhibit positive cooperativity. Under these conditions, enthalpy changes cannot explain the mechanism by which cooperativity arises, and the role of entropy changes must be considered.

(31) Williams, D. H.; Maguire, A. J.; Tsuzuki, W.; Westwell, M. S. *Science* **1998**, *280*, 711−714.

(32) Janezic, D.; Venable, R. M.; Brooks, B. R. *J. Comput. Chem.* **1995**, *16*, 1554−1566.

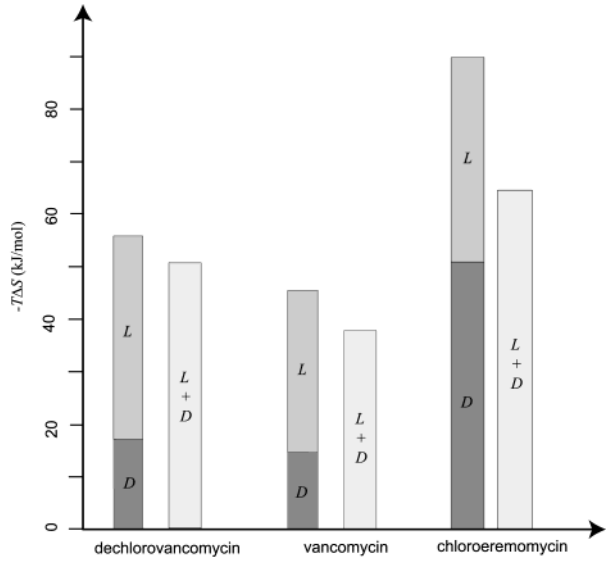

Figure 5. Interprocess cooperativity between ligand binding and dimerization. The combined entropic costs of dimerization and ligand binding (D + L) are less than the separate costs of dimerization (D) and of ligand binding (L) for all three antibiotics.

Our analyses have focused exclusively on changes in configurational entropy. Obviously, dimerization and ligand binding will also involve enthalpy changes and other types of entropy changes that cannot be evaluated with modern computational resources due to the size of this system. Overall free energy changes and cooperative behavior will be determined by the sum of all thermodynamic contributions throughout the system. However, it remains significant that configurational entropy changes *by themselves* are of sufficient magnitude to account for the experimentally observed positive cooperativity between ligand binding and dimerization.

In systems involving multivalent weak interactions, enthalpy changes typically oppose entropy changes (enthalpy−entropy compensation).[33] This tendency, and our observation that configurational entropy changes predict more cooperativity than is experimentally observed, both suggest that enthalpy changes coupled with other types of entropy changes (not taken into account in our analysis) may oppose cooperativity. When cooperativity is accompanied by structural changes, therefore, it is probably unwise to assume that the structural changes contribute in a positive manner to cooperativity without specific and explicit support for this conclusion.

The thermodynamics of cooperativity in vancomycin has been investigated calorimetrically by McPhail and Cooper.[6] For tripeptide ligand binding in D_2O at pD = 7, the enthalpy change of cooperativity was zero, while in H_2O at pH = 8, the enthalpy change opposes cooperativity. Under both of these conditions, it is clear that cooperativity is driven by positive entropy changes, and these experimental findings are consistent with the results of our calculations.

Under most other conditions, cooperativity exhibits negative overall enthalpy and entropy changes, and the role of configurational entropy is obscured by the enthalpic contribution and opposing entropic contributions. However, these results should not lead one to dismiss or discount the role of configurational entropy changes in cooperativity because the positive contribution from configurational entropy changes remains larger than the overall cooperative free energy in all cases. Hence, subtracting the configurational entropy contribution (if this were possible) would yield a unfavorable overall free energy change and create an anticooperative system.

An entropic contribution to the positive cooperativity of binding has been detected by NMR spin relaxation for the calcium ion binding protein calbindin D_{9k}.[11] Calbindin experiences a thermodynamically significant stiffening of the polypeptide backbone as it binds calcium ions and exhibits positive cooperativity.[34,35] As with the glycopeptide antibiotics, no significant changes in the conformation of calbindin are observed.

Entropically driven cooperative mechanisms may be critical to the function of much larger systems. Cooper suggested that ligand-induced modulation of periodic motions in a macromolecular system can be energetically significant[9] and that this is a plausible means of communicating the presence of bound ligand over long distances. Moreover, the enthalpy changes generally involved in the binding of small ligands are small compared to the magnitude of potential energy fluctuations one would expect in large proteins.[36] Therefore, it seems likely that large membrane proteins such as those involved in transmembrane signal transduction may depend to a significant extent on configurational entropy changes to communicate signals through a membrane. If true, the release of intracellular G_α subunits from G protein-coupled receptors upon binding an extracellular ligand[37] would be an example of ligand-induced alteration of periodic intramolecular motions, operating in conjunction with conformational changes, to yield negative cooperativity.

Acknowledgment. This work was supported by AI43412, GM54617, and the American Heart Association.

JA027780R

(33) Dunitz, J. D. *Chem. Biol.* **1995**, *2*, 709−712.
(34) Akke, M.; Bruschweiler, R.; Palmer, A. G. *J. Am. Chem. Soc.* **1993**, *115*, 9832−9833.
(35) Akke, M.; Skelton, N. J.; Kordel, J.; Palmer, A. G.; Chazin, W. J. *Biochemistry* **1993**, *32*, 9832−9844.
(36) Cooper, A. *Proc. Natl. Acad. Sci. U.S.A.* **1976**, *73*, 2740−2741.
(37) Linder, M. E.; Gilman, A. G. *Sci. Am.* **1992**, *267*, 56.